AIAA JOURNAL
Vol. 48, No. 11, November 2010

Mass Flux Sensing via Tunable Diode Laser Absorption of Water Vapor

Leyen S. Chang,* Jay B. Jeffries,† and Ronald K. Hanson‡
Stanford University, Stanford, California 94305-3032

DOI: 10.2514/1.J050544

A mass flux sensor based on line-of-sight diode laser absorption of water vapor is designed, constructed, and tested in a low-speed wind tunnel in anticipation of subsequent use in supersonic test facilities. Water vapor absorption is monitored to capitalize on its presence in air and in combustion-driven facilities as well as the availability of fiber-coupled diode lasers that access the $2\nu_1$, $2\nu_3$, and $\nu_1 + \nu_3$ absorption bands near 1.4 microns. Mass flux is determined from the product of measured velocity and density. Velocity is obtained from the relative Doppler shift of an absorption transition for beams directed upstream and downstream in the flow. Temperature is determined from the ratio of absorption signals of two transitions and is coupled with a facility pressure measurement to obtain density. The sensor exploits wavelength-modulation spectroscopy with second-harmonic detection (wavelength-modulation spectroscopy-2f) for large signal-to-noise ratios. Optimization of the modulation for 1f-normalized wavelength-modulation spectroscopy-2f (wavelength-modulation spectroscopy-2f/1f) signals for velocity sensing is presented for the first time. Criteria to select the absorption transitions are presented and the spectroscopic parameters of the needed database are determined with laboratory measurements. Using this database, the measurement of temperature is validated within 1% of thermocouple measurements in a heated cell. The velocity measurements are validated from 2.5–18 m/s with a measurement uncertainty of ±0.5 m/s in a high-uniformity wind tunnel.

Nomenclature

a	=	frequency modulation depth, cm^{-1}
c	=	speed of light in vacuum, m/s
E''	=	lower state energy of absorption transition, cm^{-1}
f	=	modulation frequency, Hz
$\bar{I}_o$	=	average laser intensity
i_o	=	linear intensity modulation amplitude
L	=	path length, cm
m	=	modulation index
N	=	exponent for pressure broadening coefficient temperature dependence
P	=	pressure, atm
S	=	linestrength, cm^{-2}/atm
T	=	temperature, K
α	=	spectral absorbance
γ	=	pressure broadening coefficient at half-width half-maximum, cm^{-1}/atm
$\Delta\nu$	=	frequency shift, cm^{-1}
$\Delta\nu_{\text{HWHM}}$	=	transition half-width at half-maximum
θ	=	crossing half-angle between two beams for Doppler shift measurement
ρ	=	density, kg/m^3
ν	=	optical frequency, cm^{-1}
$\bar{\nu}$	=	average laser frequency, cm^{-1}
ν_o	=	transition linecenter frequency, cm^{-1}
ϕ	=	lineshape function
ψ_1	=	linear intensity-frequency phase shift, rad

Presented as Paper 2010-303 at the 48th AIAA Aerospace Sciences Meeting, Orlando, FL, 4–7 January 2010; received 2 April 2010; revision received 21 June 2010; accepted for publication 6 July 2010.

*Graduate Research Assistant, High Temperature Gasdynamics Laboratory, Department of Mechanical Engineering. Student Member AIAA.

†Senior Research Associate, High Temperature Gasdynamics Laboratory, Department of Mechanical Engineering. Associate Fellow AIAA.

‡Professor, High Temperature Gasdynamics Laboratory, Department of Mechanical Engineering. Fellow AIAA.

I. Introduction

TUNABLE diode laser absorption spectroscopy (TDLAS) provides a robust, noninvasive measurement diagnostic for the harsh environments commonly experienced in high-speed or combusting propulsion flows. Gas parameters such as mole fraction, temperature, and velocity can be determined accurately with TDLAS while minimizing disturbance to the test environment. Wavelength-modulation spectroscopy (WMS) has long been used to improve the signal-to-noise of TDLAS measurements; the literature is vast and we direct the reader to reviews of the theory and experimental methods of WMS in [1–5]. TDLAS sensing with WMS has been proven in a wide variety of high-temperature and high-speed conditions [6], ranging from scramjet ground test facilities [7] to shock-heated flows [8], when conditions are sufficiently uniform along the measurement line-of-sight. TDLAS sensing of mass flux was first explored by Philippe and Hanson [9], patented for thrust measurements in 1993 [10], and used for practical measurements in a commercial turbofan (PW6000) inlet at Pratt and Whitney [11] and a full-scale Pratt and Whitney F-100 engine in an open ground test stand at the NASA Dryden Flight Research Center [12].

TDLAS measurements pass collimated laser light through an absorbing gas, and the variation of transmitted intensity with wavelength is compared with spectral models to determine gas parameters. Implementation of diode laser sensing is conceptually simple, only requiring optical access to the test gas and a laser wavelength-scanned over the range of an absorption transition. The measurement is a path integral of light attenuation along the laser beam path, and thus measurements of a flow without a uniform temperature and gas mixture require care in selecting absorption lines that minimize the influence of nonuniformities. To determine velocity, the laser beams are typically directed upstream and downstream in the flow, with a scan range sufficient to capture the Doppler shift of the absorption lineshapes. Tuning and modulation of the diode laser wavelength is normally achieved by varying the diode injection current. For wavelength-scanned WMS, a high-frequency sinusoid is superimposed upon the lower-frequency scan signal. Detecting the absorption signal at the second harmonic of the high-frequency modulation with a lock-in amplifier allows rejection of the high-frequency noise and detection on a near-zero background, thereby providing a large increase in signal-to-noise ratio.

Mass flux is an important parameter in air-breathing propulsion, and is used in calculations of inlet and combustor performance as

well as thrust and drag. Measurement of mass flux can aid in propulsion test facility operation and provide test conditions to more accurately evaluate engine performance. The sensor described in this paper is designed for ultimate use to measure mass flux in a high-temperature, supersonic flow in a combustion-driven facility, where hypersonic flight conditions are produced by expansion of hot, high-pressure air. In such facilities, the gas is typically vitiated (heated by combustion of hydrogen with oxygen-replenishment). The use of H_2O as the target species in the gas allows the sensor design to exploit mature telecommunications diode lasers in the 1.4 μm region, which can access the $2\nu_1$, $2\nu_3$, and $\nu_1 + \nu_3$ absorption bands of water vapor. Combustion product water vapor was used for TDLAS direct absorption measurements to determine velocity, temperature and density in a scramjet combustor nearly a decade ago [13]. The current sensor builds on the work of Lyle et al. [11] in which TDLAS of O_2 was used to make alternating measurements of density using wavelength-scanned direct absorption and velocity using WMS-2f. The sensor reported here extends this work to include recent developments in calibration-free WMS-2f temperature sensing [3,14,15] for simultaneous temperature and velocity measurements. The methodology for temperature and velocity measurements using WMS-2f will be discussed in detail. The sensor architecture will also be discussed, absorption transitions selected, and finally a prototype sensor assembled and tested in a wind tunnel at Stanford University with the aim of establishing sensor performance in low-speed flows. In a subsequent publication, spatially and temporally resolved measurements obtained with this mass flux sensor in a supersonic combustion-driven facility at NASA Langley Research Center (Direct Connect Supersonic Combustion Test Facility) will be presented, as well as a discussion of the influences of flow nonuniformity.

II. Theory

A. WMS-2f Spectroscopy

Although the fundamentals of WMS-2f have been studied extensively [1–5,14–16], we reproduce enough of the theory to define terms and allow the reader to understand the details of the sensor design. Our nomenclature follows that of [3,14–16]. The laser drive signal consists of a high-frequency sinusoid superimposed on a lower-frequency wavelength scan. In practice it is preferable to use a sine wave for the low-frequency scan to avoid adding higher harmonics of this scan frequency to the signal. The instantaneous laser frequency and intensity are governed by:

$$\nu(t) = \bar{\nu}(t) + a\cos(2\pi f t) \tag{1}$$

$$I_0(t) = \bar{I}_0(t) + i_0\cos(2\pi f t + \psi_1) \tag{2}$$

In Eq. (1), $\bar{\nu}(t)$ is the laser frequency [cm^{-1}] averaged over the modulation (with time dependence due to the slow-scan), f is the modulation frequency [Hz], and a is the modulation depth [cm^{-1}]. In Eq. (2), $\bar{I}_0(t)$ is the laser intensity averaged over the modulation (again with time dependence due to the slow-scan), i_0 is the linear intensity modulation amplitude, and ψ_1 is the linear phase shift between intensity and frequency. The nonlinear intensity modulation terms have been omitted as they tend to be insignificant at moderate modulation depths [16]. To successfully model the WMS signal, the parameters a, i_0, and ψ_1 must be known. These parameters are specific to a given laser current, temperature, and modulation frequency and must be measured each time these values change. The specifics of these measurements are given in more detail by Li et al. [16] and will not be covered here. The transmitted intensity I_t is governed by the Beer–Lambert relation:

$$I_t = I_0\exp(-\alpha(\nu)) = I_0\exp(-SPx_iL\phi_\nu) \tag{3}$$

where I_0 is the incident intensity, α is the spectral absorbance, S is the linestrength [cm^{-2}/atm], P is the static pressure [atm], x_i is the mole fraction of the absorbing species, L is the path length [cm], and ϕ_ν is the lineshape function at frequency ν. Equations (1–3) can now be combined to express the transmitted intensity for WMS:

$$I_t(t) = [\bar{I}_0(t) + i_0\cos(2\pi f t + \psi_1)]\exp[-\alpha(\bar{\nu}(t) + a\cos(2\pi f t))] \tag{4}$$

If the slow-scan time dependence is neglected, this function is even and can be expanded using the Fourier cosine series:

$$\exp[-\alpha(\bar{\nu} + a\cos(2\pi f t))] = \sum_{k=0}^{\infty} H_k(\bar{\nu}, a)\cos(2\pi k t) \tag{5}$$

$$H_0(\bar{\nu}, a) = \frac{1}{2\pi}\int_{-\pi}^{\pi}\exp\left[-P_iL\sum_j S_j\phi_j(\bar{\nu} + a\cos(\theta))\right]\mathrm{d}\theta \tag{6}$$

$$H_k(\bar{\nu}, a) = \frac{1}{\pi}\int_{-\pi}^{\pi}\exp\left[-P_iL\sum_j S_j\phi_j(\bar{\nu} + a\cos(\theta))\right]\cos(k\theta)\,\mathrm{d}\theta \tag{7}$$

The spectral absorbance has now been expressed as in Eq. (3), where P_i is the partial pressure of the absorbing species, S_j is the linestrength of absorption feature j, and ϕ_j is the lineshape of absorption feature j. The parameters $\bar{\nu}$ and $\bar{I}_0$ are the laser frequency and intensity averaged over the modulation at the midpoint of the slow-scan. The signal for transmitted intensity then passes through a lock-in amplifier, which consists of a mixer and a low-pass filter. The mixer multiplies the detected signal by two sinusoids of equal and arbitrary phase, producing an X and Y component:

$$X_{2f} = \frac{G\bar{I}_0}{2}\left[H_2 + \frac{i_0}{2}(H_1 + H_3)\cos\psi_1\right] \tag{8}$$

$$Y_{2f} = -\frac{G\bar{I}_0}{2}\left[\frac{i_0}{2}(H_1 - H_3)\sin\psi_1\right] \tag{9}$$

where G, the detector gain, now appears in these equations. The $2f$ signal is given by the root-sum-square of the two components:

$$S_{2f} = \sqrt{X_{2f}^2 + Y_{2f}^2} \tag{10}$$

In calibration-free WMS, the $1f$ signal is used to remove the detector gain and average laser power [14–16]. Following the same procedure, the $1f$ signal can be calculated:

$$X_{1f} = \frac{G\bar{I}_0}{2}\left[H_1 + \frac{i_0}{2}\left(H_0 + \frac{H_2}{2}\right)\cos\psi_1\right] \tag{11}$$

$$Y_{1f} = -\frac{G\bar{I}_0}{2}\left[i_0\left(H_0 - \frac{H_2}{2}\right)\sin\psi_1\right] \tag{12}$$

$$R_{1f} = \sqrt{X_{2f}^2 + Y_{2f}^2} \tag{13}$$

The $1f$-normalized $2f$ signal is now described by Eqs. (6–13), and the necessary parameters can be divided into two classes: laser modulation parameters a, i_0, and ψ_1, and spectroscopic parameters S_j and ϕ_j. The linestrength is solely a function of temperature, while the lineshape is a more complicated function of both temperature and pressure.

B. Density Measurement Methodology

Density is determined from the sensor-measured temperature and the facility pressure measurement. The $1f$-normalized WMS-2f signal can be modeled once the laser modulation and spectroscopic parameters described in the previous section have been measured. The temperature dependence of this signal is embedded in the H_i terms of Eqs. (6) and (7). The linestrength is solely a function of

temperature. The lineshape function, most commonly modeled with the Voigt profile, requires knowledge of the Doppler- and pressure-broadened half-widths. The Doppler contribution to the linewidth is a function of temperature and physical constants and does not need to be measured experimentally. The pressure-broadened contribution to the linewidth depends on broadening coefficients which must be measured (if not already known) as a function of temperature and composition. Equations (6–13) will be used to model the $1f$-normalized $2f$ signal, and the measured values will be compared with these simulations to infer temperature. This technique has been demonstrated to measure temperatures with 3% uncertainty in [14,15]. Coupling the sensor-measured temperature with an independent pressure measurement, the density ρ [kg/m^3] is determined from the ideal gas equation:

$$P = \rho RT \tag{14}$$

where P is the pressure in Pa, R is the universal gas constant for the gas mixture in J/kg K, and T is the temperature in K.

C. Velocity Measurement Methodology

If a component of flow velocity exists parallel to a beam path, an absorption feature will experience a frequency shift of its linecenter $\Delta\nu$ [cm^{-1}] given by:

$$\Delta\nu/\nu_o = U_{\text{parallel}}/c \tag{15}$$

This Doppler shift is dependent on the unshifted linecenter frequency ν_o [cm^{-1}], the speed of light c [m/s], and the component of bulk velocity parallel to the beam path U_{parallel} [m/s]. A crossed beam setup as shown in Fig. 1 is typically used to obtain the relative frequency shift. Equation (15) now becomes a function of crossing angle θ, and it can be seen from the following equation that maximum velocity resolution is obtained as the angle is maximized

$$\Delta\nu/\nu_o = 2\sin\theta \cdot U/c \tag{16}$$

Previous measurements of hypersonic velocities have applied this approach using direct absorption of water vapor and potassium [17] or nitric oxide [18]. Sensing of velocity via O_2 [9,11,19] has shown that WMS-$2f$ can provide an improvement in measurement precision and resolution. The resolution of the velocity measurement is dependent on the linecenter frequency, crossing angle, and the smallest frequency shift that can be measured. For a constant sample rate and scan rate, the frequency shift detection limit increases with laser scan amplitude since the laser must scan farther in frequency between data points. These larger scan amplitudes are necessary to resolve the lineshape of pressure-broadened features. The resolution of the $2f/1f$ lineshape for a sensor sampling at 5 MHz with a slow-scan frequency of 250 Hz and scan range of 0.35 cm^{-1} (typical width of a high-temperature H_2O absorption feature) is $7(10)^{-5}$ cm^{-1}. Assuming near-infrared diode laser absorption with a typical linecenter frequency ~7400 cm^{-1}, a frequency shift detection limit of $7(10)^{-5}$ cm^{-1}, and a crossing angle of 90°, a single-sweep velocity resolution of 2 m/s is obtained, which is roughly 0.1% uncertainty for a 1500 m/s flow and suitable for the targeted high-speed flow application. This theoretical resolution for the sensor is applicable in the limit of identical lineshapes measured on the upstream and downstream pointing beams, which are not distorted by flow nonuniformities, noise, or laser transmission/gas condition fluctuations. By fitting the lineshape and making additional Doppler shift measurements between data points, the velocity resolution can be improved to better than 1 m/s as required for a low-speed validation experiment.

D. Sensor Architecture

The details of the sensor design are shown in Fig. 1. Two lasers at λ_1 and λ_2 are modulated at f_1 and f_2 and slowly scanned with a sine wave. Light from the fiber-coupled polarization-maintained lasers is combined onto a single fiber, and then the two beams are split and directed upstream and downstream in the flow. The beams are collimated at a crossing angle of $2\theta = 90°$ through the test section and captured onto 3 MHz bandwidth InGaAs detectors. The WMS signals from multiple lasers can be demultiplexed by their modulation frequency, which allows the use of a single detector for each beam [20,21]. The signals from both beams are collected on upstream and downstream detectors and separated into signals at f_1, f_2, $2f_1$, and $2f_2$ using a software lock-in amplifier. This approach allows for simultaneous measurement of both velocity and a temperature corresponding to either beam.

E. Optimization of $2f/1f$ Lineshape for Velocimetry

Previous TDL measurements of velocity have used either direct absorption [17,18] or WMS-$2f$ [9,11,19]. The current sensing technique further improves velocimetry precision and resolution by normalizing the WMS-$2f$ signal with the WMS-$1f$ signal. From Eqs. (8–13), it is seen that the $1f$-normalized WMS-$2f$ signal is independent of detector gain and average laser intensity. This normalization has been demonstrated to improve the stability of

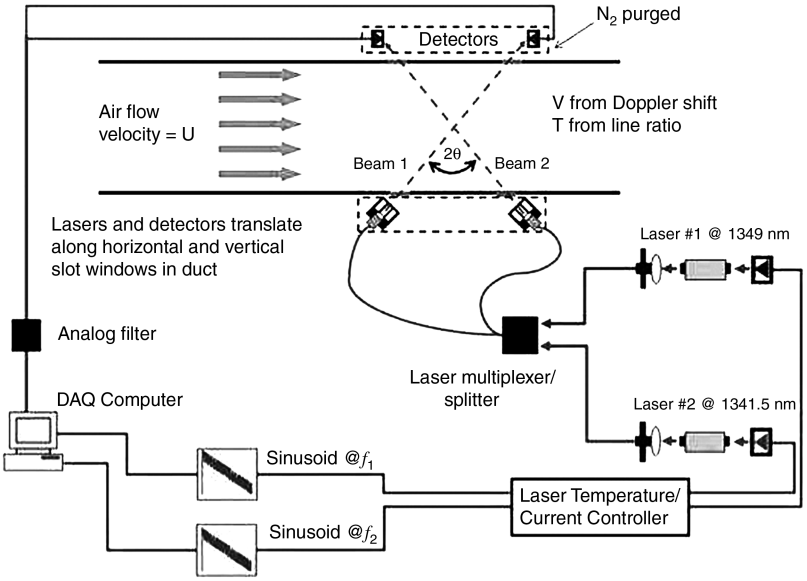

Fig. 1 Two-laser frequency-multiplexed WMS sensor for mass flux at H_2O wavelengths λ_1 and λ_2 (~1349 and 1341.5 nm). The two lasers are combined on a single fiber and then split to be directed upstream and downstream in the supersonic flow with a crossing angle 2θ. Velocity is determined from the relative Doppler shifts of the absorption lineshape, and gas temperature from the ratio of the two absorption signals.

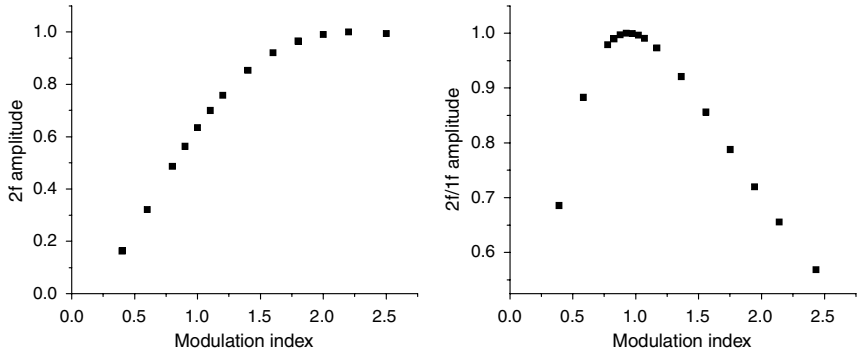

Fig. 2 Normalized amplitudes of: a) WMS-2*f* signal versus modulation index, and b) 1*f*-normalized WMS-2*f* signal versus modulation index.

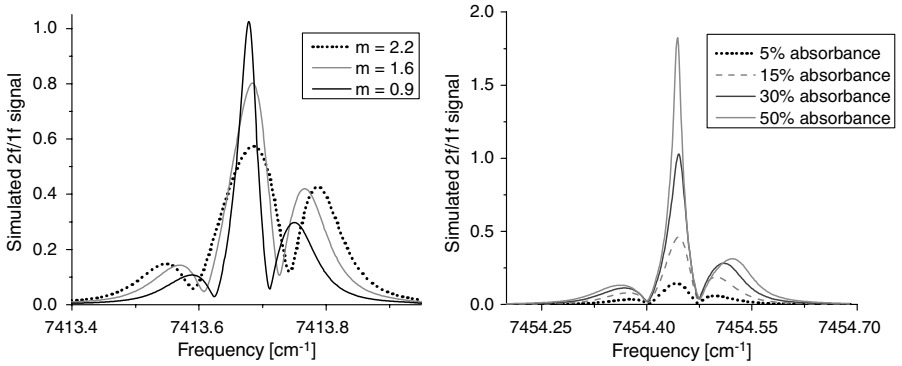

Fig. 3 Simulations of WMS-2*f*/1*f* signal: a) with varying modulation index, absorbance = 0.4, and b) with varying absorbance, $m = 0.9$.

optical sensors through resistance to transmitted laser intensity fluctuations from nonabsorption losses [14–16,22]. This feature of the WMS-$2f/1f$ signal is of great benefit for velocity sensing, where the ability to resolve Doppler shifts requires sensitive detection of the transition linecenter.

In addition to rejecting laser transmission disturbances, the WMS-$2f/1f$ signal can be sensitized to velocity by optimizing the $2f/1f$ lineshape. In particular, measurement of the Doppler shift from the difference of transition linecenters is improved when the lineshapes are tall and narrow, as may be accomplished by allowing strong absorption and by adjusting the modulation index m. When probing absorption transitions with absorbances of $>10\%$, the first harmonic of the laser transmitted intensity ($1f$) becomes significantly distorted by the absorption lineshape. The $1f$ signal reflects the first derivative of the absorption lineshape, growing taller and sharper as absorption increases. In the desired case of large absorption, normalization of the WMS-$2f$ signal by the $1f$ signal ($2f/1f$) can thus be used to generate a tall, sharply rising feature that is ideal for Doppler shift detection.

The amplitude of the $2f/1f$ lineshape is a function of the modulation index given by:

$$m = a/\Delta\nu_{\mathrm{HWHM}} \tag{17}$$

Here $\Delta\nu_{\mathrm{HWHM}}$ is the lineshape half-width at half-maximum. Previous work [7–9,14–16] has often used values of the modulation index $m \sim 2.2$ where the WMS-$2f$ signal is a maximum, as shown in Fig. 2a. However, the $2f/1f$ amplitude is a maximum for values of the modulation index $m \sim 1$, as shown in Fig. 2b. The simulations produced in Fig. 2 are for an isolated transition; in practice, the presence of neighboring lines can cause both the peak $2f$ and $2f/1f$ values to shift to slightly different modulation indices. The $2f/1f$ lineshape is sensitive to the curvature of an absorption feature; hence the specific modulation index at which the $2f/1f$ amplitude is maximized can vary slightly with different transitions and amount of absorption. However, the previously mentioned effects are minor; simulations for a wide range of transitions and degrees of absorbance show that the maximum $2f/1f$ amplitude consistently remains within the range $m = 0.9$–1, quite different from traditional use of WMS for species detection in which $m \sim 2.2$ is desired.

When $m \sim 2.2$, not only is the WMS-$2f$ signal a maximum value, but the WMS-$2f$ signal is least sensitive to the lineshape function or variations in m. Similarly when $m \sim 1$ the $1f$-normalized WMS-$2f$ signal minimizes its sensitivity to these variations; e.g., for a change in the modulation index from 0.9–1.1 the $2f/1f$ signal amplitude changes by less than 1%. In addition, when the total absorption is greater than $\sim$10%, the WMS-$2f/1f$ lineshape narrows for $m \sim 1$. The behavior of the $2f/1f$ lineshape [following Eqs. (6–13)] with varying modulation index and absorbance is illustrated in Fig. 3.

It can be seen that the $2f/1f$ lineshape at high absorbance is optimized for velocity sensing by use of a modulation index ~ 1. Optimization of the modulation index and increasing absorption have similar effects on the $2f/1f$ lineshape, causing it to increase dramatically in amplitude. For $m \sim 1$, the $2f$ amplitude is still roughly 60% of its value at $m = 2.2$; hence, the signal level is of similar strength. However, as m decreases below 0.5 or absorbance drops below 0.05, low signal levels may limit velocity resolution.

The current simulations assume that the slow-scan midpoint laser intensity ($\bar{I}_0$) is constant at all points along the lineshape. Thus the intensity variation upon which the high frequency modulation is superimposed has been neglected. A more detailed model for the scanned WMS-$2f/1f$ waveform including intensity modulation by the slow-scan is currently being developed[§]. Initial comparisons between the two models show small differences in the $2f/1f$ away from line center, though variation with absorbance and modulation index as shown above is unchanged.

[§]Strand, C. L. 2010. Private communication.

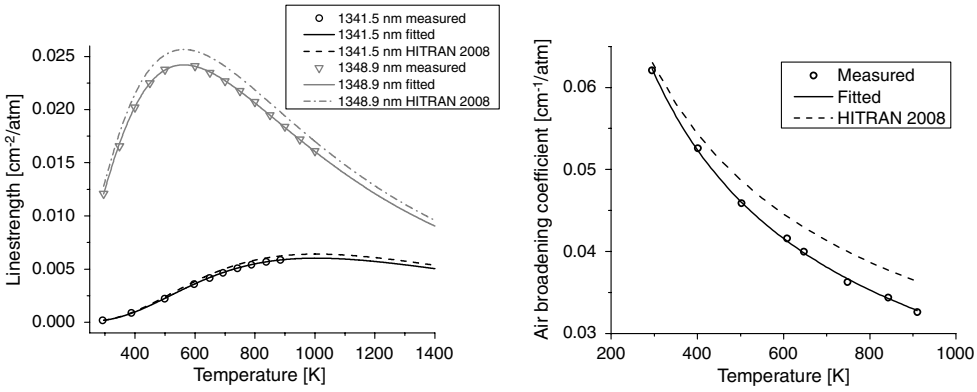

Fig. 4 Graphs of a) measured linestrength versus temperature for 1341 and 1349 nm lines, and b) measured air-broadening coefficient versus temperature for 1349 nm line. Data from HITRAN database also shown for comparison.

Previous work by Lyle et al. [19] and Philippe and Hanson [9] demonstrated that WMS-2f velocimetry offered improved signal-to-noise ratio (SNR) compared with direct absorption; here, we find that using an $m \sim 1$, the $1f$-normalized WMS-2f approach further improves the velocity resolution as demonstrated below in velocity measurements conducted in a low-speed wind tunnel at Stanford University.

F. Line Selection and Spectroscopy

Proper selection of absorption lines can reduce the effects of temperature and pressure nonuniformities along the beam path; here the criteria for selecting lines for the mass flux sensor are reviewed. These design rules are targeted toward temperature and Doppler shift velocity measurements based on absorption spectroscopy in high-temperature supersonic flows. A list of 2632 candidate water vapor transitions between 6800 and 7460 cm^{-1} (1340 and 1470 nm) where telecom diode lasers are readily available was first selected from HITRAN 2008 [23] based on a requirement of sufficient linestrength. The target supersonic test facility has a gas temperature of 600–1000 K, H_2O mole fraction of 13–25%, and an 18.7 cm pathlength. These gas conditions are then used for optimized line selection:

Absorbance greater than 0.1 was required for the facility conditions. This allows for implementation of the $2f/1f$ lineshape optimization for velocity measurement as detailed in the previous section. In addition, this absorbance level guarantees strong SNR for absorption measurements.

Minimum separation of the line centers of 0.3 cm^{-1} from the nearest neighbor is required to insure sufficient isolation and minimize distortion of Doppler-shifted features.

Difference in lower state energies of the two lines (1 and 2) was maximized as described in [24] for temperature sensitivity over the expected temperature range in the supersonic test facility.

Based on these criteria, two H_2O lines at $\lambda_1 = 1348.86$ nm ($E_1'' = 1006.12$ cm^{-1}) and $\lambda_2 = 1341.45$ nm ($E_2'' = 1962.51$ cm^{-1}) were selected. The linestrengths and air- and self-broadening coefficients (γ_{air} and γ_{self}) were measured by wavelength-scanned direct absorption in a high-uniformity heated cell at Stanford University detailed in [25]. The exponents for self-broadening N_{self} and air-broadening N_{air} temperature dependence as defined in Eqs. (18) and (19) were also measured. The experimental method detailed in [25] is applied to both linestrength and broadening coefficient measurements, with each point representing the best fit to 150 direct absorption scans

$$2\gamma_{self}(T) = 2\gamma_{self}(T_o)\left(\frac{T_o}{T}\right)^{N_{self}} \tag{18}$$

$$2\gamma_{air}(T) = 2\gamma_{air}(T_o)\left(\frac{T_o}{T}\right)^{N_{air}} \tag{19}$$

The reference temperature T_o is customarily defined to be 296 K. Figure 4 shows measurements of the linestrength and air-broadening coefficient as a function of temperature; other spectroscopic data are presented in Tables 1 and 2 and compared with values from the HITRAN [23] database.

These values provide the database needed to simulate the $1f$-normalized $2f$ signal and are used for temperature validation in the Stanford high-uniformity furnace.

III. Validation of Temperature Measurement

Water vapor temperature was measured in a quartz cell placed in the center of a three-zone furnace to provide a uniform (~1%) temperature as measured by thermocouples at the center and each end of the cell. The slow-scan frequency was set at 2 kHz and the 1349 and 1341.5 nm lasers were modulated at 190 and 255 kHz, respectively, with data collected at 5 MHz. The laser parameters i_0, a, and ψ_1 were measured at these settings to model the $1f$-normalized

Table 1 Linestrengths and self-broadening coefficients at 296 K

Line	$S_{measured}$, cm^{-2}/atm	S_{HITRAN}, cm^{-2}/atm	$\gamma_{self,measured}$, cm^{-1}/atm	$\gamma_{self,HITRAN}$, cm^{-1}/atm	$N_{self,measured}$
1348.86 nm	$1.20(10)^{-2}$	$1.28(10)^{-2}$	$2.99(10)^{-1}$	0.34	0.71
1341.44 nm	$1.73(10)^{-4}$[a]	$1.86(10)^{-4}$	$1.98(10)^{-1}$	0.25	0.56

[a]Measured by Liu et al. [25].

Table 2 Air-broadening coefficients at 296 K

Line	$\gamma_{air,measured}$, cm^{-1}/atm	$\gamma_{air,HITRAN}$, cm^{-1}/atm	$N_{air,measured}$	$N_{air,HITRAN}$
1348.86 nm	$6.21(10)^{-2}$	$6.30(10)^{-2}$	0.57	0.49
1341.44 nm	$3.23(10)^{-2}$	$3.18(10)^{-2}$	−0.16	−0.16

WMS-2f signal for a path length of 228 cm and a pressure of 14 torr of neat water vapor. Regions external to the test cell were purged with dry nitrogen to eliminate absorption from the ambient air. Before data collection, the background $2f$ and $1f$ signals are recorded; the backgrounds are then removed from the measured signals as detailed in [3]. By comparing the measured $1f$-normalized WMS-$2f$ signal to the simulated value, the temperature was inferred to within 1% of the thermocouple reading for measurements from 650–1000 K, the temperature range of interest in many high-speed propulsion flows. Similar accuracy can be obtained at lower temperatures, though other transition pairs may have preferable sensitivity in the lower temperature range. The sensor-measured temperature is compared with the thermocouple reading in Fig. 5.

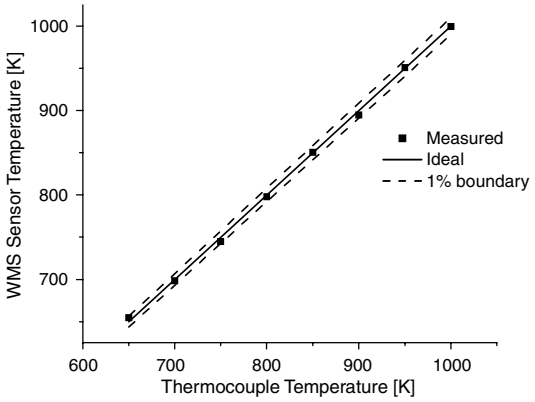

Fig. 5 Comparison of sensor and thermocouple measured temperatures in Stanford University heated cell.

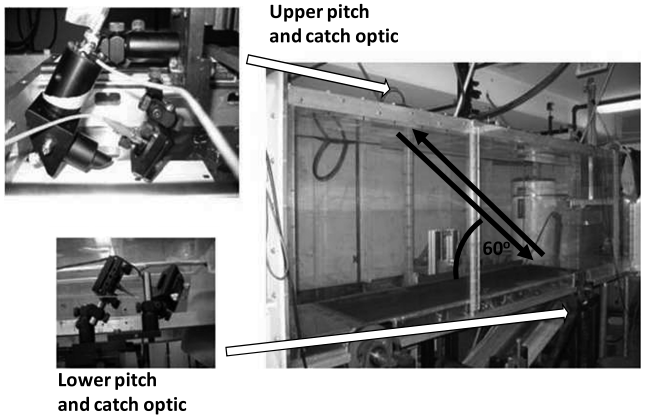

Fig. 6 Stanford University high-uniformity, low-speed tunnel with mounted sensor hardware.

IV. Validation of Velocity Measurement

A highly uniform, low-speed wind tunnel (described in detail in [26]) operating at atmospheric pressure with room temperature air and ambient humidity was used to provide a well-known flow velocity (18 m/s maximum). The tunnel is shown in Fig. 6 along with the pitch and catch optics and an illustration of the beam paths.

A different water vapor transition was selected for this particular experiment to account for the low temperature (300 K) and low water vapor mole fraction (1%). A water vapor transition near 1371 nm ($E'' = 23.8$ cm^{-1}) was used to obtain a signal for the 184 cm pathlength similar to that expected from the high-temperature, humid gas in the NASA Langley Research Center (18.7 cm pathlength, 600–1000 K, 13–25% H_2O). The optical access in this tunnel constrained the crossing angle to be $2\theta = 120°$; the slow-scan frequency was 250 Hz, the modulation frequency was 130 kHz, and the sampling rate was 5 MHz. The sensor bandwidth in this case is 500 Hz; the laser wavelength is scanned via a sine wave over the absorption lineshape twice per cycle. The velocity was determined from the Doppler shift of the $2f/1f$ lineshape, which included more than 6000 points. Use of 2000 points over a laser frequency scan range of 0.35 cm^{-1} could achieve similar velocity resolution. For subsonic velocity testing, 50 averages were used to guarantee a measurement scatter well below 1 m/s.

Data were collected for $m = 0.9$ to optimize the WMS-$2f/1f$ signal and for $m = 1.7$ to demonstrate the improvement in velocity resolution from optimizing the modulation index. Data are presented in Fig. 7, where the left panel shows measurements of time-resolved velocity (50 averages, 100 ms measurement time per data point), and the right panel shows measured velocity versus tunnel set point. This optimization of the modulation index improves the standard deviation of the measurements by 50%. This was especially important at low-speed conditions where frequency shifts are small, on the order of 10^{-4} cm^{-1}. With $m = 0.9$ the measured velocity measurements have less than a 0.5 m/s difference from the tunnel set point. The sensor architecture and modulation optimization demonstrate the capability to resolve frequency shifts less than 10^{-4} cm^{-1}, and provide confidence in application of the sensor to the supersonic regime where Doppler shifts of the absorption features are two orders-of-magnitude larger.

V. Conclusions

A mass flux sensor based on TDLAS of water vapor at 1.4 microns was designed, constructed, and tested under precisely controlled conditions at Stanford University with the goal of establishing sensor accuracy at low velocities. A new strategy to improve TDLAS velocity resolution by optimizing the modulation index for $1f$-normalized WMS-$2f$ measurements is described here for the first time. This normalization accounts for nonabsorption losses in the transmitted laser intensity, and thus reduces noise from vibration and beam steering. Line-selection criteria for the sensor design were stated and the needed spectroscopic database was measured. The

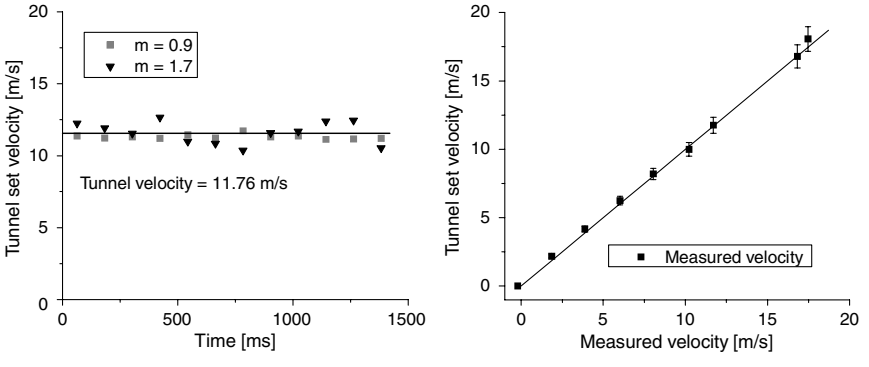

Fig. 7 Velocity measurements in Stanford high-uniformity tunnel: a) time-resolved velocity measurements for modulation index of 0.9 and 1.7, and b) measured velocity with 1 s resolution versus tunnel set point.

measurement scheme was validated in controlled laboratory environments: measurements within 1% of a thermocouple reading were performed in a heated cell at elevated temperatures, and velocity measurements within ± 0.5 m/s of the tunnel set point were obtained in a low-speed high-uniformity wind tunnel. By using newly developed guidelines for optimization of the $2f/1f$ lineshape, the velocity measurement resolution was improved substantially. These results demonstrate the potential of TDLAS sensing for accurate mass flux measurements in ground test facilities, even at low velocities. Similar precision in velocity measurements is anticipated for future applications in high-speed flows. The size, weight, and power consumption of diode laser sensors also offer the possibility for adaption to in-flight testing.

Acknowledgments

This research was supported by NASA Aeronautics program NNH06ZEA001N-HYP monitored by Glenn Diskin. The authors would like to thank Stanford University's John Eaton for use of his wind tunnel and Stanford University colleague Christopher Strand for his assistance during sensor tunnel testing.

References

[1] Silver, J. A., "Frequency-Modulation Spectroscopy for Trace Species Detection: Theory and Comparison Among Experimental Methods," *Applied Optics*, Vol. 31, No. 6, 1992, pp. 707–717. doi:10.1364/AO.31.000707

[2] Bomse, D. S., Stanton, A. C., and Silver, J. A., "Frequency Modulation and Wavelength Modulation Spectroscopies: Comparison of Experimental Methods Using a Lead-Salt Diode Laser," *Applied Optics*, Vol. 31, No. 6, 1992, pp. 718–731. doi:10.1364/AO.31.000718

[3] Rieker, G. B., Jeffries, J. B., and Hanson, R. K., "Calibration-Free Wavelength Modulation Spectroscopy for Measurements of Gas Temperature and Concentration in Harsh Environments," *Applied Optics*, Vol. 48, No. 29, 2009, pp. 5546–5560. doi:10.1364/AO.48.005546

[4] Reid, J., and Labrie, D., "Second-harmonic detection with tunable diode lasers: Comparison of experiment and theory," *Applied Physics B Lasers and Optics*, Vol. 26, No. 3, 1981, pp. 203–210.

[5] Dharamsi, N., and Bullock, A. M., "Applications of Wavelength-Modulation Spectroscopy in Resolution of Pressure and Modulation Broadened Spectra," *Applied Physics B Lasers and Optics*, Vol. 63, No. 3, 1996, pp. 283–292.

[6] Hanson, R. K., and Jeffries, J. B., "Diode Laser Sensors for Ground Testing," *25th AIAA Aerodynamic Measurement Technology and Ground Testing Conference*, AIAA Paper 2006-3441, June 2006.

[7] Liu, J. T. C., Rieker, G. B., Jeffries, J. B., Gruber, M. R., Carter, C. D., Mathur, T., and Hanson, R. K., "Near-Infrared Diode Laser Absorption Diagnostic for Temperature and Water Vapor in a Scramjet Combustor," *Applied Optics*, Vol. 44, No. 31, 2005, pp. 6701–6711. doi:10.1364/AO.44.006701

[8] Farooq, A., Jeffries, J. B., and Hanson, R. K., "Sensitive Detection of Temperature Behind Reflected Shock Waves Using Wavelength Modulation Spectroscopy of CO_2 Near 2.7 μm," *Applied Physics B Lasers and Optics*, Vol. 96, No. 1, 2009, pp. 161–173.

[9] Philippe, L. C., and Hanson, R. K., "Laser Diode Wavelength-Modulation Spectroscopy for Simultaneous Measurement of Temperature, Pressure, and Velocity in Shock-Heated Oxygen Flows," *Applied Optics*, Vol. 32, No. 30, 1993, pp. 6090–6103. doi:10.1364/AO.32.006090

[10] Hanson, R. K., "Spectroscopy-Based Thrust Sensor for High-Hyph-Speed Gaseous Flows," U.S. Patent # 5178002, 1993.

[11] Lyle, K. H., Jeffries, J. B., and Hanson, R. K., "Diode Laser Sensor for Air Mass Flux Based on Oxygen Absorption: II. Non-Uniform Flow Modeling and Aeroengine Tests," *AIAA Journal*, Vol. 45, No. 9, 2007, pp. 2213–2223. doi:10.2514/1.27683

[12] Miller, M. F., Kessler, W. J., and Allen, M. G., "Diode Laser-Based Air Mass Flux Sensor for Subsonic Aeropropulsion Inlets," *Applied Optics*, Vol. 35, No. 24, 1996, pp. 4905–4912. doi:10.1364/AO.35.004905

[13] Upschulte, B. L., Miller, M. F., Allen, M. G., "Diode Laser Sensor for Gasdynamic Measurements in a Model Scramjet Combustor," *AIAA Journal*, Vol. 38, No. 7, 2000, pp. 1246–1252. doi:10.2514/2.1094

[14] Rieker, G. B., Li, H., Liu, X., Jeffries, J. B., Hanson, R. K., "A Diode Laser Sensor for Rapid, Sensitive Measurements of Gas Temperature and Water Vapour Concentration at High Temperatures and Pressures," *Measurement Science and Technology*, Vol. 18, No. 5, 2007, pp. 1195–1204. doi:10.1088/0957-0233/18/5/005

[15] Li, H., Farooq, A., Jeffries, J. B., and Hanson, R. K., "Near-Infrared Diode Laser Absorption Sensor for Rapid Measurements of Temperature and Water Vapor in a Shock Tube," *Applied Physics B Lasers and Optics*, Vol. 89, Nos. 2–3, 2007, pp. 407–416.

[16] Li, H., Rieker, G. B., Liu, X., Jeffries, J. B., and Hanson, R. K., "Extension of Wavelength-Modulation Spectroscopy to Large Modulation Depth for Diode Laser Absorption Measurements in High-Pressure Gases," *Applied Optics*, Vol. 45, No. 5, 2006, pp. 1052–1061. doi:10.1364/AO.45.001052

[17] Wehe, S. D., Baer, D. S., Hanson, R. K., and Chadwick, K. M., "Measurements of Gas Temperature and Velocity in Hypervelocity Flow Using Diode-Laser Sensors," AIAA Paper 98-2699, June 1998.

[18] Mohamed, A., Rosier, B., Henry, D., Louvet, Y., and Varghese, P. L., "Tunable Diode Laser Measurements on Nitric Oxide in a Hypersonic Wind Tunnel," *AIAA Journal*, Vol. 34, No. 3, 1996, pp. 494–499. doi:10.2514/3.13095

[19] Lyle, K. H., Jeffries, J. B., and Hanson, R. K., "Diode Laser Sensor for Air Mass Flux Based on Oxygen Absorption: I. Design and Wind Tunnel Validation," *AIAA Journal*, Vol. 45, No. 9, 2007, pp. 2204–2212. doi:10.2514/1.26360

[20] Baer, D. S., Nagali, V., Furlong, E. R., Hanson, R. K., and Newfield, M. E., "Scanned- and Fixed-Wavelength Absorption Diagnostics for Combustion Measurements using Multiplexed Diode-Laser Sensor System," *33rd AIAA Aerospace Sciences Meeting*, AIAA Paper 95-0426, 1995;also *AIAA Journal*, Vol. 34, No. 3, 1996, pp. 489–493. doi:10.2514/3.13094

[21] Oh, D. B., Paige, M. E., and Bomse, D. S., "Frequency Modulation Multiplexing for Simultaneous Detection of Multiple Gases by Use of Wavelength Modulation Spectroscopy with Diode Lasers," *Applied Optics*, Vol. 37, No. 12, 1998, pp. 2499–2501. doi:10.1364/AO.37.002499

[22] Cassidy, D. T., and Reid, J., "Atmospheric Monitoring of Trace Gases Using Tunable Diode Lasers," *Applied Optics*, Vol. 21, No. 7, 1982, pp. 1185–1190. doi:10.1364/AO.21.001185

[23] Rothman, L. S., Gordon, I. E., Barbe, A., Benner, D. C., "The HITRAN 2008 Molecular Spectroscopic Database," *Journal of Quantitative Spectroscopy and Radiative Transfer*, Vol. 110, Nos. 9–10, 2009, pp. 533–572. doi:10.1016/j.jqsrt.2009.02.013

[24] Zhou, X., Liu, X., Jeffries, J. B., and Hanson, R. K., "Development of a Sensor for Temperature and Water Concentration in Combustion Gases Using a Single Tunable Diode Laser," *Measurement Science and Technology*, Vol. 14, No. 8, 2003, pp. 1459–1468. doi:10.1088/0957-0233/14/8/335

[25] Liu, X., Jeffries, J. B., Hanson, R. K., Hinckley, K. M., and Woodmansee, M. A., "Development of a Tunable Diode Laser Sensor for Measurements of Gas Turbine Exhaust Temperature," *Applied Physics B Lasers and Optics*, Vol. 82, No. 3, 2006, pp. 469–478.

[26] Matalanis, C. G., and Eaton, J. K., "Wake Vortex Control Using Static Segmented Gurney Flaps," *AIAA Journal*, Vol. 45, No. 2, 2007, pp. 321–328. doi:10.2514/1.25956

R. Lucht
Associate Editor